Transactions of the **14th International Conference on Structural Mechanics in Reactor Technology** (SMiRT 14), Lyon, France, August 17-22, 1997 **L01/2**

Modelling of strain rate-strain history coupling effect

Hasebe T., Imaida Y.
Doshisha University, Faculty of Engineering, Japan

ABSTRACT This study proposes microscopic hardening evolution model for describing history, rate and their coupling effects within the framework of crystalline plasticity. History and rate effects, respectively, are modelled based on junction formation with forests, and the dislocation dynamics. Unzipping model is additionally introduced to describe the coupling effect based on the inertia effect of moving dislocation. Applicability of the models are verified through comparisons with experimental observations.

1. INTRODUCTION

Hardening behavior of crystalline materials is substantially controlled by development of dislocation substructure and its interaction with mobile dislocation. The former is responsible for strain history effect especially under nonproportional loading, while the latter for strain rate effect. Constitutive modelling for each effect has been widely made, however, their coupling effect has not been fully discussed to date to the authors' knowledge. Reasonable as well as accurate modelling of hardening characteristics under such complex conditions are required for realizing effective system for numerical simulation–combined structural design.

The present study purposes to develop hardening evolution model of crystalline materials which can describe complicated behavior associated with strain history and strain rate. General form of hardening evolution equation is proposed in which two models are implemented corresponding to strain history and strain rate effects[1–3]. History–rate coupling effect model is additionally introduced based on unzipping of dislocation segments caused by inertial effect. Stress responses under several nonproportional cyclic strain paths and pre–torsion/compression static/dynamic loading are simulated and compared with experimental observations reported so far, and the validity of the proposed models are extensively discussed.

2. CONSTITUTIVE EQUATION

Analysis based on the crystalline plasticity theory is composed of two sequential procedures, i.e., localization and homogenization, which are interconnected by microscopic

constitutive equation. The above procedures are mathematically expressed, respectively, by,

$$\tau^{(\alpha)}=tr(\boldsymbol{P}^{(\alpha)}\sigma)$$
$$\dot{\varepsilon}^{p}=\sum_{\alpha=1}^{N}\boldsymbol{P}^{(\alpha)}\dot{\gamma}^{(\alpha)} \tag{1}$$

where $\boldsymbol{P}^{(\alpha)}$ denotes direction tensor defined by $\boldsymbol{P}^{(\alpha)}=1/2(\boldsymbol{s}^{(\alpha)}\boldsymbol{m}^{(\alpha)}+\boldsymbol{m}^{(\alpha)}\boldsymbol{s}^{(\alpha)})$. Here, $\boldsymbol{s}^{(\alpha)}$, $\boldsymbol{m}^{(\alpha)}$are unit vectors for slip direction and slip plane normal, respectively.

Based upon phenomenological internal state variable theory, we employ the following general form of the microscopic constitutive equation.

$$\dot{\gamma}^{(\alpha)}=f\left(\frac{|\tau^{(\alpha)}-\Omega^{(\alpha)}|}{K^{(\alpha)}}\right) \tag{2}$$

where $K^{(\alpha)}$, $\Omega^{(\alpha)}$ are drag and back stress state variables, respectively. The back stress generally describes resistance against dislocation motion provided by local obstacles such as forests and precipitates, producing short range stress field. The back stress, on the other hand, represents increase in dislocation resistance to motion caused by pileups at global obstacles such as grain boundaries, producing long range stress field. We focus here on evolution of the former, the drag stress, which mainly responsible for hardening.

2. HARDENING EVOLUTION EQUATION

Evolution equation for drag stress $K^{(\alpha)}$ depicts time evolution of hardening within a crystal, so that the hardening law gives the general form as[4],

$$\dot{\tau}^{(\alpha)}=\sum_{\beta=1}^{N}h_{\alpha\beta}|\dot{\gamma}^{(\beta)}| \tag{3}$$

Here $h_{\alpha\beta}$ expresses matrix with 12×12 components for FCC metals. This paper proposes the following general form of evolution equation for the drag stress.

$$\dot{K}^{(\alpha)}=(\dot{\pi}^{(\alpha)}+\dot{\omega}^{(\alpha)})\cdot Q_{\alpha} \quad (\textit{no sum on } \alpha) \tag{4}$$

where Q_{α} is hardening ratio, which expresses strain history effect reflecting development of dislocation substructure based on junction formation with forests. $\pi^{(\alpha)}$ and $\omega^{(\alpha)}$ correspond to stress components associated with immobile/weakly mobile, and mobile dislocations, respectively. The former is associated with internal stress field provided by accumulation and development of dislocation substructures, generally described by Eq.(3). The latter term describes effective stress produced by resistance against moving dislocation, thus giving strain rate effect.

We postulate that forest dislocations are formed during the previous loading, and the dislocation generated in the subsequent loading interacts with them and forms junction[1,2]. Introducing interaction matrix $f_{\alpha\beta}$, we have,

$$Q_\alpha = \frac{1}{N}\sum_{\beta=1}^{N}(1+f_{\alpha\kappa}S_{\kappa\beta})$$
$$S_{\alpha\beta} = \delta_{\alpha\beta}\tanh\left(\frac{W_p^{(\beta)}}{(W_p)_{sat}}\right)\cdot\Gamma^{(\alpha)} \quad (5)$$

where $S_{\alpha\beta}$ indicates strain history matrix being a function of previous work in each slip system $W_p^{(\beta)}$. Q_α takes unity when there is no strain history. $\Gamma^{(\alpha)}$ indicates apparent reduction of the history effect caused by inertial effect of moving dislocation, which will be discussed later.

The general form of $\omega^{(\alpha)}$ in Eq.(4) has been suggested by the authors[3] covering a wide range of strain rate from 10^{-4} to $10^{5}s^{-1}$.

$$\dot{\omega}^{(\alpha)} = \dot{\omega}_1(\ ln\dot{\gamma}^{(\alpha)},\ \rho,\ T\ ) + \dot{\omega}_2(\dot{\gamma}^{(\alpha)},\ \rho,\ T\ ) \quad (6)$$

First and second terms of the right-hand side of Eq.(6) respectively describes thermally activated and viscous drag mechanisms[3]. The present study employ the simplest form of Eq.(6) given by,

$$\dot{\omega}^{(\alpha)} = A_1\cdot ln(1+A_2\dot{\gamma}^{(\alpha)}) + B\dot{\gamma}^{(\alpha)} \quad (7)$$

where A_1, A_2 and B are material constants.

3. HISTORY-RATE COUPLING EFFECT

As experimental results demonstrated[3], a significant coupling should exist between strain history and strain rate effects. This phenomena is considered to be caused by unzipping of dislocation segments based on the inertial effect. Figure 2 illustrates the inertial effect and the unzipping behavior. Small Peierls potential in FCC metals leads to sufficient acceleration of dislocation between obstacles under high strain rate loading, which consequently produces the inertial effect. The dislocation segment pinned by pair of obstacles are instantaneously curved by the inertial effect, and mechanically breaks through the obstacles when the bent angle exceeds the critical value(Fig.2(a)). The unpinned dislocation segment induces additional unpinning in the neighborhood; this is called as "unzipping behavior"(Fig.2(b)).

Here we assume the simplest form of $\Gamma^{(\alpha)}$ for describing the "unzipping behavior" as,

$$\Gamma^{(\alpha)} = 1 - \frac{<\xi^{(\alpha)} - \xi_{th}>}{\xi_{cr}} \quad (8)$$

where $\xi^{(\alpha)}$ is defined as functions of both kinetic energy of moving dislocation and potential energy accumulated to the pinned dislocation segment. ξ_{th} and ξ_{cr}, respectively, express threshold and critical values of $\xi^{(\alpha)}$. Variation of $\Gamma^{(\alpha)}$ with $\xi^{(\alpha)}$ is shown in Fig.3: the value of $\Gamma^{(\alpha)}$ decreases with increasing $\xi^{(\alpha)}$, which corresponds to apparent reduction of strain history effect with increasing strain rate or accumulated strain. ξ_{th}

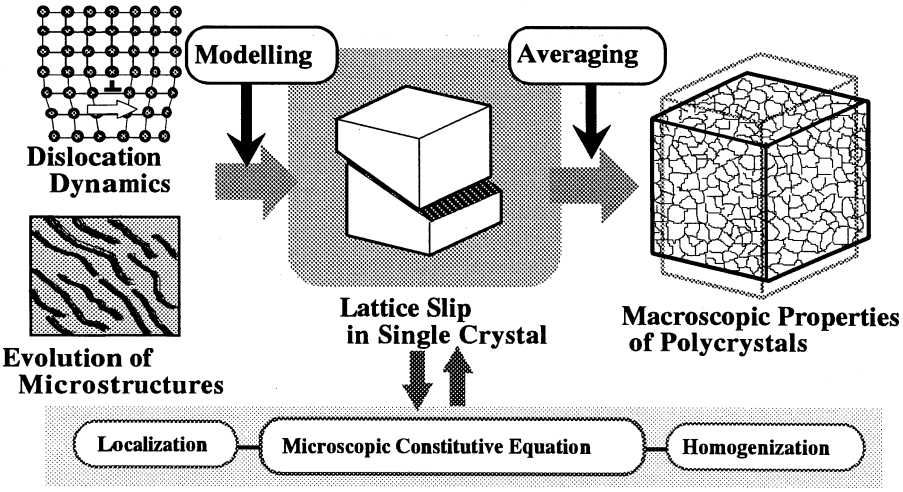

Fig.1 Flow of analysis based on crystalline plasticity

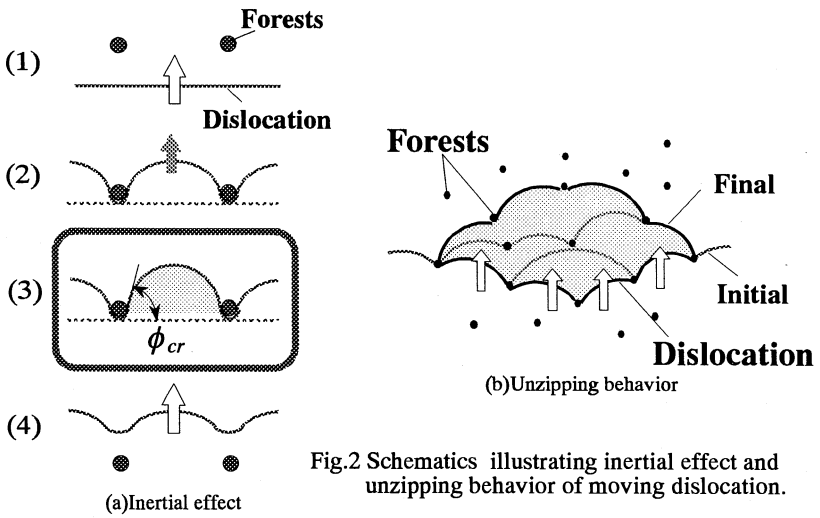

Fig.2 Schematics illustrating inertial effect and unzipping behavior of moving dislocation.

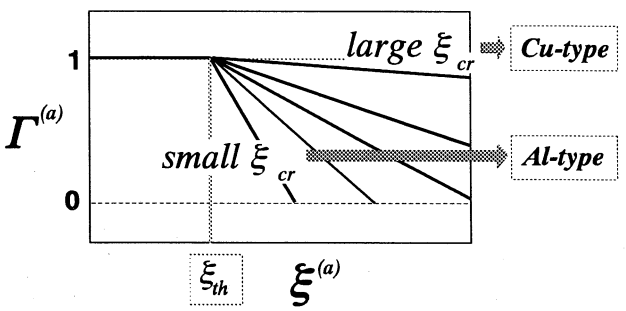

Fig.3 Variation of coupling function Γ with ξ for changing ξ_{cr} .

reflects density and distribution of obstacles, whereas ξ_{cr} is dominated by nature of obstacle and its strength against dislocation motion. Since the paper mainly considers forests as the obstacle, ξ_{cr} should be given as a function of stacking fault energy(S.F.E.). Variation of $\xi^{(a)}$–$\Gamma^{(a)}$ relation with ξ_{cr} is also shown in Fig.3. Small ξ_{cr} corresponding to metals with large S.F.E. yields sharp drop of $\Gamma^{(a)}$ with increasing $\xi^{(a)}$, and vice versa for the case of large ξ_{cr}. Al and Cu are the typical for the former and the latter, respectively.

4.ANALYTICAL RESULTS AND DISCUSSION

4.1 *Strain History Effect*

The history effect model is firstly applied to nonproportional loading assuming $\omega^{(a)}$=0. Polycrystal analysis is made under constant strain assumption[1,2] for three representative strain paths, i.e., cruciform, rectangular and circle. The cruciform path is a typical case for alternative tension–torsion loading, while square and circular paths are those for 90° out–of–phase loading. Figure 4 compares flow stress at saturation normalized by that for push–pull between the present analysis and experiments reported by Banellal et al.[5] for type 316 stainless steel at room temperature. It has been found that the out–of–phase type loading exhibits the largest cyclic hardening compared with alternative types such as cruciform strain path[5], as long as strain path is limited in biaxial states[6]. The analytical results successfully estimate the above trend, and quantitatively agree with experimental results.

Transition of nonproportionality is simulated by using stair–step strain paths, and comparison is made with experiments[5] in Fig.4(b). Experimental observation indicated that strain paths with many steps exhibit similar hardening response to that under in–phase loading, and the additional hardening rapidly becomes significant as the number of steps decreases. The present analysis shows good agreement with the experimentally observed trend. The stress responses in the present model are shown in Fig.5(a), demonstrating high nonproportionality corresponding to those of strain paths. Plastic strain history shown in Fig.5(b), on the other hand, exhibits different trend from that of the stress history. The plastic strain response for four–step path is very close to that of an in–phase loading, regardless the highly non–proportional stress response. The nonproportionality of plastic strain history increases as the number of stair–steps decreases. The above results agree with experimental observations by Doong, Socie, et al.[7]. Therefore, we can conclude that the present model has the intrinsic ability to describe the hardening behavior under complicated non–proportional loadings.

4.2 *History–Rate Coupling Effect*

The proposed model is applied also to static as well as impact compression following pre–torsion in order to examine the ability for describing the history–rate coupling effect. In this case, time–independent constitutive equation is used[3] as the framework to omit strain rate effect come out of rate sensitivity coefficient. Polycrystal composed of 500 grains is considered based on stress constant model.

The authors have reported typical experimental results representing the coupling effect for Al and Cu[3] as follows. For static compression, strain history effect introduced by

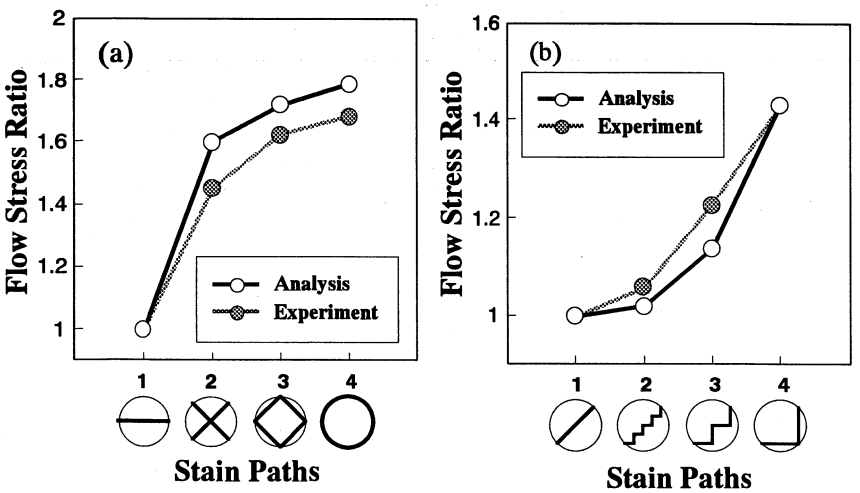

Fig.4 Comparison of flow stress ratio under nonproprtional loading with experimental results after Benellal, et al..

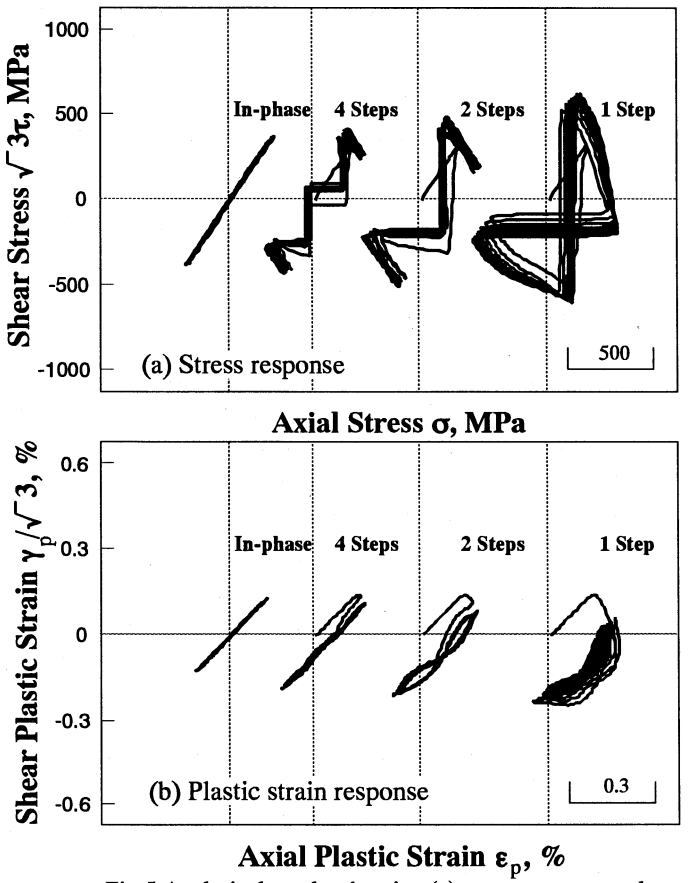

Fig.5 Analytical results showing (a)stress response and (b)plastic strain response for stair-step strain paths.

pre-torsion strain is observed at yielding for Al, but it vanishes at large strain region. In Cu, on the other hand, flow stress increase at yielding remains even when the strain becomes large. Under impact compression, the temporarily increased flow stress at yielding, observed in Al under static compression, completely disappears, whereas the strain history effect becomes more significant for Cu. Thus the history-rate interaction is strongly material-dependent. Evidently, these results cannot be simply explained by simple superposition of strain history and rate effects.

Analytical results corresponding to the above experiments are shown in Fig.6. One can see that the present model qualitatively expresses not only the history-rate coupling effect for both low and high strain rates but also their material dependency.

Figure 7 shows analytical stress-strain responses under strain rate change tests. As can be understood from the figure, the present proposed model can also describe the "strain rate history effect" for FCC metals.

5. CONCLUSION

(1)Evolution equation of hardening are proposed to describe both strain history and strain rate effects. The former is based on dislocation interaction with forests, while the latter is derived from dislocation dynamics.
(2)Unzipping model based on inertial effect of moving dislocation against randomly distributed forests are proposed for expressing history-rate coupling effect, and is introduced in the above evolution equation.
(3)Applicability of the proposed models are verified through comparisons with experimental observations.

REFERENCES

1. Hasebe, T., Y. Imaida, & H. Nakamoto 1995. Flow stress of FCC metals under unsteady transient loadings. *Dynamic Plasticity and Structural Behaviors (Proc. Plasticity '96)*, Osaka, Japan. 825-828. Gordon and Breach Publishers.
2. Hasebe, T. & Y. Imaida 1995. Hardening behavior of FCC crystals under non-proportional loadings. *Proc. 1995 Japan-Sino Bilateral Symp. on High Temperature Strength of Materials*, Nagaoka, Japan. 135-140.
3. Hasebe, T., Y. Imaida, H. Nakamoto & K. Shibahara 1996. Strain rate and strain history effects on hardening behavior of FCC metals under dynamic loading -constitutive modelling based on the crystalline plasticity-. *Proc. AEPA '96*, Eds. T. Abe, T. Tsuta; 357-362. Pergamon.
4. Khan, A. S. & S. Huang, 1995. *Continuum Theory of Plasticity*. Wiley-Interscience.
5. Benallal, A., P. LeGallo and D. Marquis 1989. An experimental investigation of cyclic hardening of 316 stainless steel and of 2024 Aluminium alloy under multiaxial loadings. *Nucl. Eng. Des.* **114**, 345-353.
6. Cailletaud, G. 1992. A micromechanical approach to inelastic behavior of metls. *Int. J. Plasticity*. **8**, 55-73.
7. Doong, S. H., D. F. Socie & I. M. Robertson 1990. Dislocation substructures and nonproportional loading. *Trans. ASME, J. Eng. Mater. Technol.*, **112**, 456-464.

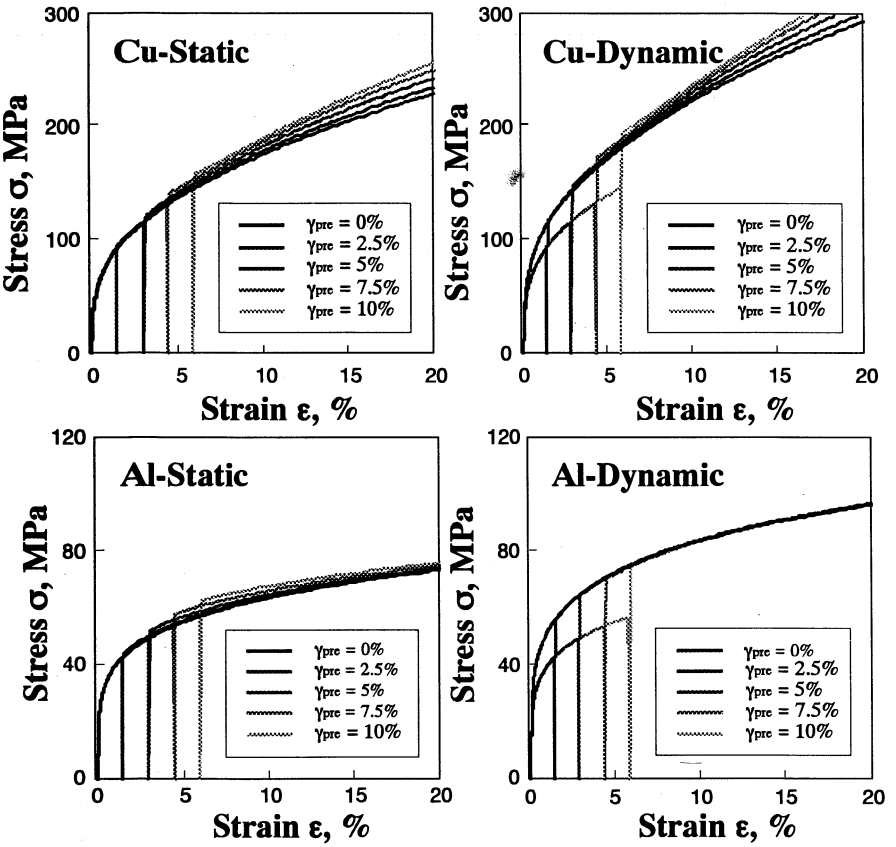

Fig.6 Analytical results demonstrating history-rate coupling effect together with its material dependency.

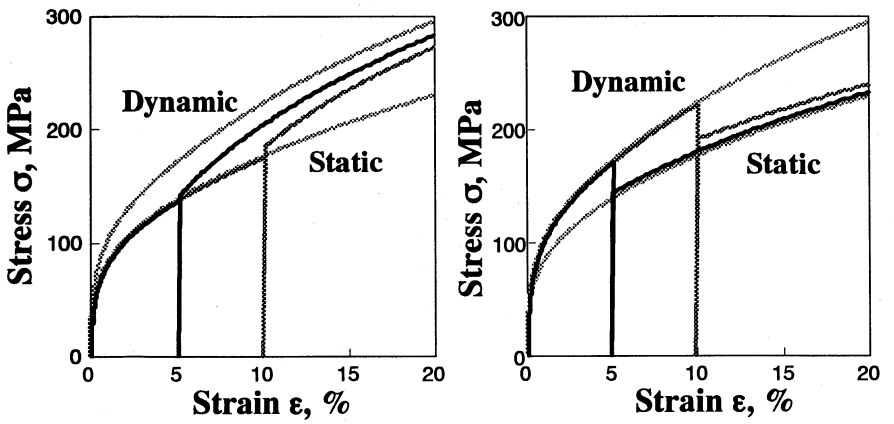

(a) Static→Dynamic (b) Dynamic→Static

Fig.7 Analytical results showing strain rate history effect for (a)static to dynamic, and (b)dynamic to static.